Title

LINGO3 regulates mucosal tissue regeneration and promotes TFF2 dependent recovery from colitis

Journal

Scandinavian Journal of Gastroenterology, 56(7)

ISSN

0036-5521

Authors

Zullo, Kelly M
Douglas, Bonnie
Maloney, Nicole M
et al.

Publication Date

2021-07-03

DOI

10.1080/00365521.2021.1917650

Peer reviewed

HHS Public Access

Author manuscript

Scand J Gastroenterol. Author manuscript; available in PMC 2021 December 06.

Published in final edited form as:

Scand J Gastroenterol. 2021 July ; 56(7): 791–805. doi:10.1080/00365521.2021.1917650.

LINGO3 regulates mucosal tissue regeneration and promotes TFF2 dependent recovery from colitis

Kelly M. Zullo[1], **Bonnie Douglas**[1], **Nicole M. Maloney**[1], **Yingbiao Ji**[1], **Yun Wei**[2], **Karl Herbine**[1], **Rachel Cohen**[1], **Christopher Pastore**[1], **Zvi Cramer**[3], **Xin Wang**[3], **Wenjie Wei**[4], **Ma Somsouk**[5], **Li Yin Hung**[1,2], **Christopher Lengner**[3], **Michael H. Kohanski**[6,7], **Noam A. Cohen**[6,7,8], **De'Broski R. Herbert**[1,2]

[1]Department of Pathobiology, University of Pennsylvania School of Veterinary Medicine, Philadelphia, PA 19104

[2]Department of Medicine, Division of Experimental Medicine, University of California, San Francisco, San Francisco, CA 94143, USA.

[3]Department of Biomedical Sciences, University of Pennsylvania School of Veterinary Medicine, Philadelphia, PA 19104

[4]Department of Ophthalmology, Perelman School of Medicine, University of Pennsylvania, Philadelphia, PA 19147

[5]Department of Pathology, University of California, San Francisco, San Francisco, CA 94143, USA.

[6]Department of Otorhinolaryngology—Head and Neck Surgery, Perelman School of Medicine at The University of Pennsylvania, Philadelphia, PA 19104

[7]The Corporal Michael J. Crescenz VA Medical Center Surgical Service, Philadelphia, PA 19104

[8]Monell Chemical Senses Center, Philadelphia, PA 19104

Abstract

Recovery of damaged mucosal surfaces following inflammatory insult requires diverse regenerative mechanisms that remain poorly defined. Previously, we demonstrated that the reparative actions of Trefoil Factor 3 (TFF3) depend upon the enigmatic receptor, leucine rich repeat and immunoglobulin-like domain containing nogo receptor 2 (LINGO2). This study examined the related orphan receptor LINGO3 in the context of intestinal tissue damage to determine whether LINGO family members are generally important for mucosal wound healing and maintenance of the intestinal stem cell (ISC) compartment needed for turnover of mucosal epithelium. We find that LINGO3 is broadly expressed on human enterocytes and sparsely on discrete cells within the crypt niche, that contains ISCs. Loss of function studies indicate that LINGO3 is involved in recovery of normal intestinal architecture following dextran sodium sulfate

Corresponding Author: De'Broski R. Herbert Ph.D., 3800 Spruce St. Old Vet 369E, Philadelphia, PA 19104, Tel: (215) 898-9151, Fax (215) 206-8091, debroski@vet.upenn.edu.

Conflicts statement

We declare no conflicts of interest with this manuscript

(DSS)-induced colitis, and that LINGO3 is needed for therapeutic action of the long acting TFF2 fusion protein (TFF2-Fc), including a number of signaling pathways critical for cell proliferation and wound repair. LINGO3-TFF2 protein-protein interactions were relatively weak however and LINGO3 was only partially responsible for TFF2 induced MAPK signaling suggesting additional un-identified components of a receptor complex. However, deficiency in either TFF2 or LINGO3 abrogated budding/growth of intestinal organoids and reduced expression of the intestinal ISC gene leucine-rich repeat-containing G-protein coupled receptor 5 (LGR5), indicating homologous roles for these proteins in tissue regeneration, possibly via regulation of ISCs in the crypt niche. Thus, we propose that LINGO3 serves a previously unappreciated role in promoting mucosal wound healing.

Keywords

LINGO3; TFF2; intestinal stem cells; DSS colitis; Lrg5; mucosal barriers

Introduction

Intestinal epithelial cells (IECs) are comprised of multiple lineages that form a nutrient absorptive barrier organized into an intricate villus/crypt architecture covered by a mucus biogel matrix that restricts microbial translocation [1–5]. Defects in the mechanisms protecting this mucosal barrier predispose individuals to develop Inflammatory Bowel Diseases (IBD) such as Crohn's disease and Ulcerative colitis [6–8]. IBD pathogenesis is largely driven by microbial-induced inflammation resulting in persistent bloody diarrhea, abdominal pain, bowel obstructions, abscesses and fistulas, which cost approximately $6.3 billion annually to treat [9]. However, of the approximately 3.1 million Americans diagnosed with IBD [10], it is projected that only a fraction of patients achieve and sustain remission with current biologics [11]. Therefore, a more in-depth understanding of the molecular mechanisms that promote GI mucosal barrier integrity is critical to identify new targets for disease management.

The relapsing-remitting nature of IBD emphasizes the critical importance of tissue regenerative pathways in disease resolution. Normally, tissue regeneration within the intestine is continuous and rapid; mature IECs are replaced every 3 to 5 days by a highly active intestinal stem cell (ISC) compartment. ISCs express the leucine-rich repeat-containing G-protein coupled receptor 5 (LGR5) within the crypt based columnar cells (CBCs) that support homeostatic turnover and regeneration after injury[12–14]. Additionally, a +4 subset of ISCs express *Bmi1*, *Lrig1*, *HopX*, *Tert* and also contributes to repair of the intestinal epithelium after injury [15]. The survival, proliferation, and cell fate determination of ISCs are critical to the maintenance and repair of mucosal layer. These processes are controlled by signaling pathways involving WNT- -catenin, EGF, NOTCH, BMP families, as well as interleukins (IL) such as IL-22, IL-4 and IL-13 [15–18]. However, the signals that drive the ISC expansion following tissue disruption by mechanical, chemical or inflammatory insults remain incompletely understood. Secreted glycoproteins in the Trefoil factor family (TFF) have been long recognized as mediators of mucosal wound healing. These proteins promote epithelial survival, proliferation, and the directed movement

of epithelial cells across denuded areas of basement membrane post-injury. TFF proteins accumulate at the leading edge of mucosal wounds and are highly expressed in ulcer associated cell lineage (UACL) glands [19, 20]. TFF proteins can serve as ligands for a number of different receptors to effect various functions. For example, in the pancreas, TFF2 promotes cell proliferation by acting as a ligand of the CXCR4 receptor and activating the map kinase pathway [21]. TFF2 can also associate with β-catenin to promote proliferation and cell survival [22]. Whether TFF proteins have any direct role within the ISC niche is unclear. There is co-expression of TFF2 and Lrg5 found in the upper gastrointestional tract [23], suggesting that TFF2 could play some role to promote cell proliferation in the ISC niche.

We recently demonstrated that intestinal tissue recovery from dextran sodium sulfate (DSS)-induced colitis relied upon the ability of TFF3 to serve as an activating ligand for leucine rich repeat and immunoglobulin-like domain containing nogo receptor 2 (LINGO2) [24]. This study investigated whether a related LINGO family member, LINGO3 could also promote tissue repair after mucosal injury, potentially through interactions with other TFF family members. We found that DSS-induced colitis in LINGO3 deficient mice resulted in severe defects in intestinal tissue recovery as compared to wildtype (WT) controls. Consistent with a potential role in ISC biology, LINGO3 deficiency abrogated *Lgr5* expression during intestinal healing and impaired the self-renewing capacity of small and large intestinal organoids. Although LINGO3-TFF2 interactions were of moderate affinity, LINGO3 was still required for exogenous TFF2 agonist treatment to accelerate healing following DSS. These findings support a previously unappreciated role for LINGO3 in tissue repair, and suggest that the LINGO family may have a conserved role in mucosal regeneration.

Materials and Methods

Human tissue and immunostaining.

Archived rectosigmoid biopsy samples were from the SCOPE cohort at the University of California, San Francisco (UCSF). The UCSF Committee on Human Research reviewed and approved the SCOPE study (IRB# 10–01218), all participants provided written informed consent. Rectosigmoid biopsies were obtained by sigmoidoscopy approximately 10–30 cm from the anal verge. Human sinonasal polyp samples were obtained from patients undergoing sinonasal surgery for the management of their chronic rhinosinusitis with informed consent and full approval of the University of Pennsylvania Institutional Review Board (Protocol #800614). Tissue sections from Human sinonasal polyps and rectosigmoid (normal) were fixed in formalin and paraffin embedded for sectioning. The sections were deparaffinized and antigen was retrieved using an electric pressure cooker (Nesco PC6–25P) in a low-pH Citrate Buffer. Human tissues were stained with the following primary antibodies: anti-LINGO3 (Santa Cruz sc-247444, raised in goat) and anti-TFF2 (Peprotech: 500-P312, raised in rabbit). Primary antibodies visualized using Alexa Fluor conjugated secondary antibodies (AffiniPure F(ab')$_2$ Fragment Donkey Anti-Rabbit and Anti-Goat IgGs, Jackson ImmunoResearch). DAPI was used to visualize nuclei. Detection of fluorescence was observed under Cy2, Cy3, and Cy5 filters on a Leica Inverted

Microscope DMi8 S Platform and a Leica DM6000B microscope with an automated stage coupled with a Leica DFC350FX camera. We normalized exposure times and fluorescence intensities to appropriate control images. We photographed fluorescent channels separately, merged them together and overlaid them atop the corresponding images.

Mice.

All animal procedures were approved by the Institutional Animal Care and Use Committees (IACUC) at University of California, San Francisco (protocol #AN109782–01), and the University of Pennsylvania (protocol #805911). Both Tff2 and LINGO3 KO mice were generated at the University of California, San Francisco. All experiments were performed at the University of Pennsylvania unless otherwise specified, where both transgenic lines and wildtype (WT) (C57bl6) were bred and housed specific-pathogen free barrier conditions.

Nasal epithelial cell culture and wound healing assay.

This experiment was performed using established protocols [25–28]. Briefly, primary murine nasal epithelial cells were grown for 7 days as submerged cultures and for 2 weeks at air liquid interface in transwells. On day 21, monolayers were wounded in a cross pattern with a sterile pipet tip (1mm width) and treated daily on the apical side with 10 ng/ml recombinant human TFF2 (Peprotech) or 1xPBS (Mock). Cultures were rinsed with 1X PBS prior to TEER measurement. Serial measurements of TEER (Ohms-cm2) were taken using an EVOM (World precision instruments) and the cup/transwell insert adapter.

Dextran sodium sulfate (DSS) model.

All experiments used six to ten-week-old wildtype (WT) or LINGO3 KO C57BL/6 female mice bred in house and cohoused for four weeks. Colitis was induced using 2.5% Dextran Sulfate Sodium Salt (w/v, 0216011080, MP-Biomedicals LLC Solon, OH) in autoclaved drinking water for 6 days. Fresh solution was provided on day 3, on day 6 mice were returned to normal water and monitored until necropsy on day 10, when colons were measured and dissected for histology or quantification of *Lgr5* mRNA. For TFF2 treatment, mice were administered either 150 ng of TFF2-Fc (1ng/uL) or Fc (1 ng/uL) via intraperitoneal injection on Day 3, 6, 9 post 2.5% DSS treatment. Body weight, appearance, stool consistency/diarrhea, and fecal occult blood (Fisherbrand™ Sure-Vue™ Fecal Occult Blood Slide Test System, ThermoFisher Scientific, Inc., Waltham, MA, USA) were recorded daily from tattooed animals and used to determine the Disease Activity Index (DAI). The DAI is a cumulative score (maximum 12) determined from: appearance score (1 for each display of lack of grooming, piloerection, awkward gait, hunched posture, and lack of mobility), diarrhea score (0 Normal stool, 1 soft stool 2 loose formed stools, and 3 watery fecal matter), rectal bleeding score (0 no blood, 1 minor bleeding, and 2 gross rectal bleeding), and fecal occult blood score (0 Negative, 1 Mild amount of blood, and 2 excessive presence of blood).

Histological staining and pathology of mouse colon.

On the 10th day following the start of DSS administration, mice were euthanized and colons extracted. Colon tissue was either opened longitudinally, flushed with ice-cold PBS

to remove feces and formalin fixed as “swiss rolls” or 1–2 cm of the distal colon. All subsequent histology was performed by the Veterinary Comparative Pathology Core at the University of Pennsylvania and the tissues were evaluated by a clinical pathologist who was blind to genotype and treatment. Colon tissues were stained with hematoxylin and eosin (H&E), periodic acid Schiff stain (PAS) to identify goblet cells, and immunohistochemistry against pERK1/2 (CST #4370), Caspase-3 (CST #9661), p-STAT3 (CST #9145S), β-catenin (CST #9582), and Ki-67 (Thermo Scientific RM-9106-S). For quantification of β-catenin the region of interest was outlined and percent threshold area was measured using MetaMorph microscopy automation and image analysis software. All images were normalized using a standard set for hue, saturation, and intensity (72,255,255, respectively). A Leica widefield microscope was used for imaging.

Histopathological analysis by the pathologist focused on assessing the chronic mucosal changes (inflammatory and proliferative) of the mid and distal colorectal tract present in each sample. In some samples, the pathological picture was very heterogeneous combining severe ulcerative lesions with nearly normal mucosal segments. This finding reflects the typical multifocal nature of the ulcerative and inflammatory lesions induced by repeated DSS administration. The extensive loss of mucosal glands observed in some of the samples precluded in part the evaluation of pathological changes specifically affecting the mucosal crypts including inflammation and hyperplasia.

The pathologist evaluated the samples to determine the Inflammation Score (Fig.3D), using published methods [29, 30]. Briefly, each section was scored for severity (0 = no abnormal immune cell infiltration, 1 = mild: low density infiltration confined to mucosa, 2 = moderate: moderate or higher density infiltration in mucosa and/or low to moderate density in mucosa and submucosa, 3 = severe: high density infiltration in submucosa and/or extension into muscularis, 4 = marked: high density infiltration with frequent transmural extension) and for extent of section affected by inflammation (0 = none, 1 = up to 25%, 2 = up to 50%, 3 = up to 75%, and 4 = up to 100%). These values are multiplied together to derive the Inflammation Score for each section (maximum of 16). Crypt loss (Fig. 3E) was also evaluated by the pathologist using a scoring system modified from [31, 32] (0 = normal mucosa, 1 = shortening of basal one-third of crypts with slight inflammation and edema in lamina propria, 2 = loss of basal two-thirds of crypts and moderate inflammation in lamina propria, 3 = loss of all epithelium, severe inflammation in lamina propria and/or submucosa, but with surface epithelium still remaining, and 4 = loss of all epithelium, severe inflammation in the lamina propria, submucosa, and muscularis, and exudate containing cell debris, inflammatory cells, fibrin and mucus covers the damaged mucosa).

Intestinal organoid cultures.

Crypts were isolated from mouse small intestinal jejunum with modifications indicated [13, 33]. Briefly, the small intestines and colons of WT and LINGO3 KO mice were removed, opened longitudinally and washed with Ca^{2+}-Mg^{2+}-free Hank’s balanced salt solution (HBSS). Villi were scraped off using a coverslip under a dissecting microscope, and the tissue was incubated in 5mM EDTA in HBSS for 30 mins at 4°C on an orbital shaker. Residual villi were removed with further washing. The crypts were separated from

the basal membrane by vigorous pipetting in 0.5% BSA in HBSS and then filtered through a 70-μm cell strainer. Crypts were pelleted at 250 × *g* (5 min, 4°C) and resuspended in complete crypt culture medium (Advanced DMEM/F12 [Thermo, 12634–010], 10 mM HEPES [IVT, 15630–080], 1x penicillin/streptomycin [IVT, 15140–122], 1x gentamycin [Gibco, 15750–500], 1x N2 Supplement [IVT, 17502–048], 1x B27 Supplement [IVT 17504–044], 1mM N-Acetyl-cysteine [Sigma, A9165–5g], 50ng/mL recombinant mouse epidermal grown factor [IVT, PMG8041], 100ng/mL mNOGGIN [peprotech, 250–38], 1 μg/mL R-spondin 1 [R&D, 3474-RS-050], 5mM CHIR99021 [Stemgent 04–0004], to a final volume of 2%). Approximately 100–300 crypts per well were then embedded in 80% Matrigel/20% complete crypt culture media in pre-warmed 48-well flat bottom plates and incubated for 15 min at 37°C. Embedded enteroids were cultured in 200 μL of complete crypt culture media added at 37°C and 5% CO_2 with media changed every 2–3 days. Organoids were imaged using an inverted Nikon eclipse (TE2000-U) widefield microscope at 4x, 10x, and 20 x on day 3, 5, and 7 of growth.

Soluble ligand binding assay.

Purified murine IgG (RayBiotech), murine recombinant TFF2 (Peprotech) and SDF1a (R&D systems) were labeled with Alexa Fluor 647 dye using the Alexa Fluor 647 protein labeling kit (A30009, Molecular Probes) per manufacturer's directions. HEK293 cells were maintained in DMEM medium (Invitrogen) supplemented with 10% fetal bovine serum (Invitrogen) and 1% penicillin-streptomycin (Invitrogen) at 37°C with 5% CO2. HEK293 cells were seeded at 1×10^6/well and incubated at 37°C with 5% CO2 overnight before transfection with 3–6ug of plasmids pCMV3-mLINGO3-GFP, pCMV3-mLINGO2-GFP or pCMV3-mCXCR4-GFP using FuGENE HD DNA transfection reagent (Promega) based on manufacturer's instructions. 24h post transfection, cells were incubated with either PBS or 3ug of Alexa Fluor 647 labeled soluble ligands for 16h at 4°C. Cells expressing GFP and Alexa Fluor 647 positive were identified by flow cytometry.

Co-immunoprecipitation.

2.4×10^6 CHO cells were transfected with 24 μg pCMV6:LINGO3:Flag (MR215769, Origene) or pCMV6 entry plasmids. After incubation cells were washed twice with PBS, lysed with 300 μL digitonin extraction buffer, and protein concentration was measured using BCA assay kit (Invitrogen). Around 0.6 mg total protein was mixed with 20μg purified TFF2-Fc (Ray Biotech) or Fc (Ray Biotech) and precleared with control agarose resin for 1 hr at 4°C. The lysate samples were then precipitated with 40 μl protein A/G agarose (Invitrogen) overnight at 4°C. The immunoprecipitation (IP) complex was washed with TBS for 5 times and eluted with 4× SDS loading buffer at 95°C. The IP elutes along with whole cell lysates were immunoblotted with rabbit anti-FLAG (1:400) followed by incubation with goat anti-rabbit IgG Cy5 (1:1000). More detail in supplemental methods.

Statistics.

Statistical analyses were performed using GraphPad Prism version 7.0 (GraphPad). A two-tailed Student's T test or ANOVA was used where appropriate.

Results

LINGO3 is expressed in human mucosal tissues

To characterize LINGO3 expression in human intestinal mucosa across different subjects, formalin-fixed paraffin embedded (FFPE) rectosigmoid biopsies were immunostained with commercially available, validated anti-human LINGO3pAb. Data show that LINGO3 (green) localized to the apical and basolateral surfaces of colonic enterocytes (Figure 1 B,C,E,F). In some cases, LINGO3 was more intensely expressed at the basolateral surface (Figure 1B). LINGO3 was additionally localized in a sparse punctate pattern along the crypt base, with approximately 1–3 cells per crypt in a position consistent with the ISC niche (Figure 1F). The expression of LINGO3 protein in the ISC niche is consistent with reports indicating *Lingo3* mRNA expression on $LGR5^{+}$ cells and transit-amplifying cells [34–36]. As others have shown [37, 38], we also found LINGO3 expression in nasal polyp tissues obtained from patients with chronic rhinosinusitis. The pattern of expression was again distributed across apical and basolateral surfaces within these tissues (Figure 1 H–K). Strikingly, co-immunostaining of these tissues with anti-human TFF2 mAb revealed that TFF2 localized to the apical surface in a globular manner consistent with the mucin layer. There was no staining in the isotype matched Ab controls of intestinal or nasal polyp tissue, confirming specificity of the primary antibodies (Figure 1 A, D, G). These findings indicate that LINGO3 and TFF2 are expressed in close proximity in mucosal tissues, which includes the intestinal microenvironment.

Loss of LINGO3 impairs epithelial cell recovery following injury

We thought that because LINGO3 is found in mucosal tissues in close proximity to TFF2 it could play a role in mucosal tissue repair, as we previously found for LINGO2 and TFF3 [24]. To test this possibility in the upper airway, we performed sterile scratch wound assays using mature cultured sinonasal epithelial cells from WT and LINGO3 KO. Changes in trans-epithelial electrical resistance (TEER) values over time were used as a proxy for recovery of barrier integrity (Figure 2A). There was no difference in rate of recovery between WT and LINGO3 KO epithelia after injury. TFFs promote wound repair [25, 39–41] and can interact with LINGO family proteins [24] to augment recovery of mucosal barrier integrity [42] [43]. We therefore thought that addition of rTFF would aid wound healing in WT cultures, but might still be impaired in the absence of LINGO3, which was the case. Following scratch wounding, TEER rebound values were accelerated in rTFF2-treated WT cultures, but the addition of rTFF2 had no impact on the recovery rate of LINGO3 KO sinonasal epithelia (Figure 2a). This data suggested that TFF2 promoted an acceleration of epithelial monolayer recovery, at least partially, through LINGO3 dependent mechanisms.

Next, to investigate the role for LINGO3 in the recovery of intestinal epithelial cells following tissue injury, we used a protocol that distinguished the acute injury vs. regenerative phases of DSS colitis [44]. Age-matched, co-housed cohorts of WT and LINGO3 KO mice were administered 2.5% DSS *ad libitum* in the drinking water over 6 days, then returned to normal drinking water and monitored 4 days thereafter for weight rebound and disease activity index (DAI) over the course of the injury and recovery phases.

During the early injury phase of DSS treatment (0–5 days) there were no significant differences between strains in weight change or DAI score between LINGO3 KO and WT mice (Figure 2B,C). In contrast, in the recovery phase from days 6–10 (DSS removed), LINGO3 KO mice continued to lose weight and had increased DAI scores, in contrast to WT mice that exhibited stabilized weight and reduced DAI score that returned to normal by day 10 (Figure 2B,C). Colons of LINGO3 KO mice were shorter than WT on day 10 (Figure 2D). Furthermore, LINGO3 KO mice had worsened pathology as determined by histological evaluation on day 10 (Figure 2 E–G). Taken together, these findings suggest that LINGO3 is critical for healing following injury to mucosal epithelial tissues, particularly in the intestinal tract.

To establish whether TFF2 would heal damaged colonic mucosa in a manner dependent upon LINGO3, we asked whether therapeutic administration of a long acting TFF2 construct (TFF2-Fc fusion protein) would show any protective efficacy in DSS-treated WT and LINGO3 KO mice. Cohorts of each strain were intraperitoneally administered 150 ng of TFF2-Fc or Fc alone at d3, d6, and d9 following 2.5% DSS administration (see Supplemental Figure 1A for purification of TFF2-Fc). TFF2-Fc improved weight recovery, reduced DAI scores and increased colon lengths in the WT strain compared to Fc alone treatment (Figure 3A–C). However, with the exception of mild improvement in DAI score on the last day, these beneficial effects of TFF2-Fc treatment were not observed in LINGO3 *KO* mice (Figure 3 A–C). Histological evaluation of colon tissue at day 10 post-DSS administration revealed that TFF2-Fc treatment promoted faster recovery of goblet cell-rich, crypt architecture lacking ulceration with reduced immune cell infiltration in WT, but not LINGO3 KO groups (Figure 3 F–G). TFF2-Fc treatment was also associated with preservation of colon length, significantly reduced inflammation and crypt loss scores in WT, but not LINGO3 KO groups (Figure 3 C–E). Taken together, these findings indicate that LINGO3 is required for TFF2-mediated mucosal epithelial healing.

LINGO3 is only partially responsible for TFF2 signaling during recovery from injury

TFF2 signaling may promote intestinal healing by enhanced cell proliferation or inhibition of apoptotic cell death, and LINGO3 may be required for of this effect. Therefore, we used immunohistochemistry of the colon biopsies from WT and LINGO3 KO mice, +/− TFF2-FC treatment, to assess changes in markers for intracellular signaling associated with cell proliferation, such as the phosphorylation of ERK1/2 in MAPK signaling [21, 26, 45], the phosphorylation of STAT3 which has been associated with TFF3 activity [41, 46, 47], expression of β-catenin [22], and the S-phase protein Ki-67, a general marker for cell proliferation [47, 48]. We also stained for cleaved caspase 3 to assess apoptotic cell death, as TFF2 signaling has been linked to modulation of apoptotic signaling [39] (pERK1/2 shown in Figure3F–H, and all others shown in Figure 4).

For all of the markers associated with cell proliferation, except pERK1/2, we found significant differences between injured WT and LINGO3 KO mouse tissues in the control condition (Fc only) (Figure 3F–H, Figure 4A–F), with less immunoreactivity in KO tissues, suggesting that either LINGO3 may be involved in these signaling cascades or worsened pathology in the KO mice is associated with this staining pattern. We also found

that TFF2-Fc treatment in WT significantly increased pERK1/2+ cells and significantly decreased the number of positive pSTAT3, Ki-67 cells and levels of β-catenin, but did not exert these significant effects in LINGO3 KO tissues (Figure 3F–H, Figure 4A–F). Further, under control conditions, cleaved caspase 3+ cells were not significantly different between the genotypes, and TFF2-FC treatment in WT also had no significant effect on cleaved caspase 3+ cell numbers. However, within the TFF2-FC treated groups, there were significantly more caspase 3+ cells in the LINGO3 KO tissues than in WT (Figure 4 G,H). Taken together, these data demonstrate that TFF2 accelerated colonic tissue recovery, which required LINGO3 expression and was associated with MAPK activation. The failure of LINGO3 KO to recover from injury, was also associated with decreased STAT3 and β-catenin activation that could not be reversed by TFF2-Fc treatment. LINGO3 deficiency increased IEC apoptosis despite TFF2-Fc treatment. This indicated that only certain functions of TFF2 were LINGO3 dependent, whereas the predominance of the biological defects evident in LINGO3 KO mice could not be reversed by TFF2-Fc treatment.

LINGO3 and TFF2 are both required for intestinal stem cell activity

Because LINGO3 was found expressed at the crypt base of human rectal biopsy tissue, we questioned whether LINGO3 deficiency somehow affected ISC function. We evaluated mouse colon tissues under basal conditions and post-DSS treatment for mRNA expression levels of *Lgr5*, a gene known to be necessary for colonic recovery following DSS treatment [49]. Lgr5 expression was significantly lower in LINGO3 KO mice as compared to WT under both basal and post-DSS treatment conditions (Figure 5A). TFF2-Fc treatment did not have any impact on *Lgr5* expression (data not shown).

Because of the complex *in vivo* setting where microbial contents and inflammatory cytokines can have a major impact upon ISC activity [15], we employed an intestinal organoid culture system to test whether LINGO3 had a cell-intrinsic effect on organoid growth/budding and expression of *Lgr5* [13]. Small intestinal organoids were grown over 7 days and evaluated for budding and overall size as surrogates for ISC activity (Figure 5B). Curiously, organoids grown from small intestine of both LINGO3 and TFF2 KO mice had a 2–4 fold reduction in budding and size when compared to WT (Figure 5C), which was not explained by overall difference in cell area (Figure 5D). *Lgr5* mRNA levels in LINGO3 KO and TFF2 KO organoids were significantly lower than WT (Figure 5E). LINGO3KO organoids had decreased *Tff2* expression levels, while TFF2 KO organoids had an additional decrease in *Tff3* expression (Figure 5F). In contrast, the phenotype of colonic LINGO3 KO organoids had increased budding compared to WT, whereas TFF2 KO organoids had no difference relative to WT (Figure 5G,H). By day 7 however, both LINGO3 KO and TFF2 KO colonic organoids had a spontaneously loss of their 3D architecture and became flattened and 2D when compared to WT organoids (Figure 5G). These data demonstrate that both small intestinal and colonic organoids from LINGO3 KO and TFF2 KO mice have a marked dysregulation in architecture as compared to WT.

TFF2 weakly interacts with LINGO3

LINGO3 is an orphan receptor with no known ligand, but given the similarities in localization and function between TFF2 and LINGO3, we postulated that TFF2 perhaps

interacted with LINGO3. To determine if TFF2 and LINGO3 would interact at the cell membrane, flow cytometry was used to establish whether over-expression of LINGO3-GFP, LINGO2-GFP, or CXCR4-GFP fusion constructs transfected into HEK293 cells would allow binding to soluble ligand molecules conjugated to Alexa Fluor 647: recombinant (r)TFF2 (TFF2–647), Ctrl Ig (IgG-647), or rSDF-1 (SDF-1–647) (Figure 6A illustrates transfection scheme, Supplemental Figure 1B shows gating strategy for flow cytometry). SDF-1 is a known binding partner with high affinity for CXCR4, so this pairing serves as a strong positive control signal [21]. There was a 6–10 fold higher frequency of TFF2–647-bound to LINGO3-GFP transfectants than to TFF2-LINGO2 transfectants or TFF2-CXCR4 transfectants, respectively (Figure 6D–F). There was negligible binding with IgG-LINGO3 control and no Alexa Fluor 647 signal with PBS-LINGO3 negative control (Figure 6B–C). The frequency of TFF2-bound to LINGO3-GFP transfectants was slightly lower than the frequency of double positive SDF-1–647 CXCR4-GFP cells, which had the highest frequency of binding in this assay as expected for a known receptor-ligand interaction (Fig. 6D,G). As a complementary approach, we performed co-immunoprecipitation experiments to test whether Flag-tagged LINGO3 would bind to affinity-purified TFF2-Fc-fusion protein (Figure 6H,I). To do this, CHO cells were transfected with either empty vector or Flag-tagged LINGO3 for 72hrs, lysed and complexed with soluble Fc or TFF2-Fc followed by protein G pulldown and immunoblotting against the Flag epitope. A moderate signal was detected in the TFF2-LINGO3 sample, but not with Fc only, indicating a weak interaction (Figure 6H,I). Thus, we conclude that TFF2 is not a direct ligand for LINGO3 and that additional un-identified molecules are needed for their interaction.

Discussion

This study demonstrates a critical role for the orphan transmembrane receptor LINGO3 as a previously unrecognized mediator of mucosal wound healing. In human tissues, LINGO3 is constitutively expressed in IECs lining the human colonic mucosa under normal conditions, including un-identified cells within the ISC crypt niche, and is expressed on the airway epithelium in nasal polyps. Studies using LINGO3 deficient mice subjected to the DSS colitis model reveal that LINGO3 is particularly important during the regenerative phase of tissue healing following colitis, and the presence of LINGO3 was required for the long acting TFF2-Fc protein to exert therapeutic effects and activate MAPK signaling. The loss of LINGO3 was also associated with reduced activation of STAT3 and β-catenin pathways, less cell proliferation, and increased apoptosis in the context of injury, which were not affected by TFF2-Fc treatment. Given that LINGO3 staining occurred in within the ISC crypt niche, we evaluated expression levels of the ISC marker *Lgr5* and found it to be reduced in LINGO3 KO mice. Organoid experiments also indicated that both LINGO3 and TFF2 contribute to expression levels of *Lgr5* and appropriate budding and cellular architecture. While our investigations did not reveal that the reparative cytokine TFF2 binds directly to LINGO3, the weak binding interactions identified by immunoprecipitation and the partial overlap in function been LINGO3 and TFF2 suggests that these molecules function in similar regenerative pathways operating at the mucosal surfaces, potentially involving the ISC niche.

Our data support a hypothesis that LINGO3 promotes wound healing, which is strikingly consistent with the established paradigm of TFFs regulating wound repair. TFFs regulate epithelial biology through restitution, cellular migration, regulation of tight junction proteins, and inhibition of epithelial cell apoptosis [25, 39–41]. Combined with our recent work demonstrating the importance for TFF3-LINGO2 interactions, the present work suggests that LINGO proteins may possess conserved roles in tissue repair. Although LINGO1 has been implicated in inhibition of axon regeneration, there is a dearth of information on the biological role(s) for LINGO2–4. Therefore, our work is highly significant as there is no data on LINGO3 signaling or transcriptional regulation.

Within the cytoplasmic tail of LINGO3 there are serine and tyrosine residues that have been predicted to be possible phosphorylation targets by kinases belonging to the MAPK and AKT signaling cascades, kinases implicated in TFF2 signaling and tissue regeneration [21, 26]. TFF2-Fc treatment during DSS induced colitis successfully accelerated recovery from damage caused by DSS. This treatment required intact LINGO3 expression in order to fully activate MAPK/ERK pathways as observed in WT mice, suggesting that while TFF2 and LINGO3 may not directly interact, these two molecules may promote similar signaling pathways.

While most of our data support the idea that LINGO3 is required for TFF2-Fc's therapeutic function, one caveat and seemingly incongruous cleaved caspase 9 findings bear further discussion. A major caveat of our histology related to intracellular signaling cascades (pERK1/2, pSTAT3, β-cateinin), apoptosis (cleaved caspase 9), and cell proliferation (Ki67) is that we only examined the end timepoint, 10 days post DSS, and did not have non-colitis LINGO3 KO controls for comparison, in the interest of limiting the number of animals used. Given that TFF2-FC treatment seems to accelerate healing in this model and that LINGO3 loss impairs healing, we are likely not capturing peak apoptosis and proliferation in all the groups. Healing from colitis can be associated with reduced apoptosis, including assessment by caspase 9 protein expression [50]. While we did not observe that in our histological data for WT TFF2-FC vs FC treated mice, we did appear to have an overall elevation in caspase 9 associated with LINGO3 KO. We interpret the trend of increase between WT and LINGO3KO FC treated controls, along with the significant increase in TFF2-FC treated LINGO3 KO (Figure 4H) as being due more to the loss of LINGO3 than the TFF2-FC treatment itself, given that there was no statistically significant difference between LINGO3 KO mice with or without TFF2-FC treatment. This would be in agreement with the poor recovery of LINGO3 KO mice from DSS colitis (Figure 1). The fact that caspase 9 is not significantly reduced in the WT TFF2-FC vs FC may be because by day 10 we are past the peak in apoptotic cell loss in WT DSS colitis, given the low numbers of positive cells in either group. This interpretation may be supported by the significant increase in proliferation seen in the WT FC group at this timepoint. At day 10, we may have exceeded the optimal the window of resolved apoptosis/maximal proliferation in the TFF2-Fc treated WT mice that have accelerated recovery, but just seeing post-apoptotic proliferation and initial healing in WT Fc controls.

TFFs have been implicated as putative treatments for IBD [51]. Interestingly, the pro-inflammatory pathways that drive IBD pathogenesis such as TNF and NF-κB can inhibit

transcription of TFF3, suggesting that pro-inflammatory cytokine production antagonizes the wound healing functions of TFF3 [52]. Both TFF2 and TFF3 have been shown to suppress pro-inflammatory cytokine production from immune cells including tissue macrophages of various organs [53, 54]. While treatment with recombinant TFF2 is protective in rats and dogs during experimental colitis [55] and is known to reduce leukocyte recruitment in inflamed tissues [56], there have been no clinical studies evaluating TFF2 as a putative therapy for IBD. Interestingly, LINGO3 deficiency impaired STAT3 activation in a TFF2-Fc independent manner which clearly indicates that LINGO3 can function in epithelial repair mechanisms independent of TFF2.

Some features of the LINGO family of receptors bear structural homology to transmembrane receptors involved in Wnt signaling for the stem cell niche including Leucine Rich Repeat Containing G Protein-Coupled Receptors 4–6 [57]. Proteins of this family bind R-spondin family members and regulate Wnt signaling within intestinal crypts to drive survival and cellular proliferation. When Lgr5 and Lgr4 are deleted *in vivo*, intestinal crypts are lost, and proliferation is decreased. Additionally, work from Liu *et al* further demonstrates that Lgr4 deficient mice have reduced Paneth and $Lgr5^{+}$ cells and have worsened DSS-induced colitis and a defect in proliferation [58]. This phenotype is remarkably similar to LINGO3 KO mice that have reduced intestinal *Lgr5* expression, show defective intestinal organoid growth and have significantly impaired ability to recover from DSS-induced colitis. Moreover, organoids derived from small intestines of LINGO3 KO mice do not bud and grow normally as observed with organoids grown from the small intestines of WT mice. Colonic organoids deficient in LINGO3 lose their 3-D architecture, flattening their appearance in a manner consistent with epithelial-mesenchymal transition (EMT) [59–62]. These phenotypes could be partially explained by dysregulated Wnt signaling or defective stem cells functions. Taken together, it is tempting to speculate that LINGOs are a family of reparative proteins that have functional roles in Wnt signaling and maintenance of stem cells [63–65]. This would be entirely consistent with the immunostaining pattern of LINGO3 within the human colon in regions of the intestinal stem cell crypt niche.

In sum, the work presented here has identified LINGO3 as serving a necessary role in the healing phase of DSS colitis. This work suggests that LINGO3 partially confers TFF2 responsiveness in promoting tissue recovery at the intestinal mucosal barrier interface. Further, we provide indirect evidence that LINGO3 is important for maintaining the ISC niche. Clearly, there remain many unanswered questions for future study in this area that include: 1) identity of LINGO3 ligand(s), 2) LINGO3 regulation on distinct intestinal epithelial cell lineages, and 3) whether LINGO3 forms a multi-protein signaling complex as was shown for LINGO1. In this regard, this work lays the foundation for future studies focused on understanding the immunoregulation of LINGO and other family members.

Supplementary Material

Refer to Web version on PubMed Central for supplementary material.

Acknowledgements

D.R.H. is supported by NIH (AI095289, GM083204, UO1AI125940) and the Burroughs Wellcome Fund. We thank Dr. Heather Rossi for her editorial assistance.

References

1. Bevins CL and Salzman NH, Paneth cells, antimicrobial peptides and maintenance of intestinal homeostasis. Nat Rev Microbiol, 2011. 9(5): p. 356–68. [PubMed: 21423246]
2. Knoop KA and Newberry RD, Goblet cells: multifaceted players in immunity at mucosal surfaces. Mucosal Immunol, 2018. 11(6): p. 1551–1557. [PubMed: 29867079]
3. Kim YS and Ho SB, Intestinal goblet cells and mucins in health and disease: recent insights and progress. Curr Gastroenterol Rep, 2010. 12(5): p. 319–30. [PubMed: 20703838]
4. Mailliard ME, Stevens BR, and Mann GE, Amino acid transport by small intestinal, hepatic, and pancreatic epithelia. Gastroenterology, 1995. 108(3): p. 888–910. [PubMed: 7875494]
5. Chen L, Tuo B, and Dong H, Regulation of Intestinal Glucose Absorption by Ion Channels and Transporters. Nutrients, 2016. 8(1).
6. Muise AM, et al. , Polymorphisms in E-cadherin (CDH1) result in a mis-localised cytoplasmic protein that is associated with Crohn's disease. Gut, 2009. 58(8): p. 1121–7. [PubMed: 19398441]
7. Scharl M, et al. , Protection of epithelial barrier function by the Crohn's disease associated gene protein tyrosine phosphatase n2. Gastroenterology, 2009. 137(6): p. 2030–2040 e5. [PubMed: 19818778]
8. Hassan SW, et al. , Increased susceptibility to dextran sulfate sodium induced colitis in the T cell protein tyrosine phosphatase heterozygous mouse. PLoS One, 2010. 5(1): p. e8868. [PubMed: 20111595]
9. Kappelman MD, et al. , Direct health care costs of Crohn's disease and ulcerative colitis in US children and adults. Gastroenterology, 2008. 135(6): p. 1907–13. [PubMed: 18854185]
10. Dahlhamer JM, et al. , Prevalence of Inflammatory Bowel Disease Among Adults Aged >/=18 Years - United States, 2015. MMWR Morb Mortal Wkly Rep, 2016. 65(42): p. 1166–1169. [PubMed: 27787492]
11. Cote-Daigneault J, et al. , Biologics in inflammatory bowel disease: what are the data? United European Gastroenterol J, 2015. 3(5): p. 419–28.
12. Barker N, et al. , Identification of stem cells in small intestine and colon by marker gene Lgr5. Nature, 2007. 449(7165): p. 1003–7. [PubMed: 17934449]
13. Sato T, et al. , Single Lgr5 stem cells build crypt-villus structures in vitro without a mesenchymal niche. Nature, 2009. 459(7244): p. 262–5. [PubMed: 19329995]
14. Metcalfe C, et al. , Lgr5+ stem cells are indispensable for radiation-induced intestinal regeneration. Cell Stem Cell, 2014. 14(2): p. 149–59. [PubMed: 24332836]
15. Gehart H and Clevers H, Tales from the crypt: new insights into intestinal stem cells. Nat Rev Gastroenterol Hepatol, 2019. 16(1): p. 19–34. [PubMed: 30429586]
16. Pinto D, et al. , Canonical Wnt signals are essential for homeostasis of the intestinal epithelium. Genes Dev, 2003. 17(14): p. 1709–13. [PubMed: 12865297]
17. Sato T, et al. , Paneth cells constitute the niche for Lgr5 stem cells in intestinal crypts. Nature, 2011. 469(7330): p. 415–8. [PubMed: 21113151]
18. Hardwick JC, et al. , Bone morphogenetic protein 2 is expressed by, and acts upon, mature epithelial cells in the colon. Gastroenterology, 2004. 126(1): p. 111–21. [PubMed: 14699493]
19. Wright NA, et al. , Trefoil peptide gene expression in gastrointestinal epithelial cells in inflammatory bowel disease. Gastroenterology, 1993. 104(1): p. 12–20. [PubMed: 8419234]
20. Longman RJ, et al. , Coordinated localisation of mucins and trefoil peptides in the ulcer associated cell lineage and the gastrointestinal mucosa. Gut, 2000. 47(6): p. 792–800. [PubMed: 11076877]
21. Orime K, et al. , Trefoil factor 2 promotes cell proliferation in pancreatic beta-cells through CXCR-4-mediated ERK1/2 phosphorylation. Endocrinology, 2013. 154(1): p. 54–64. [PubMed: 23183167]

22. Zhou Y, Zhang Y, and Wang J, Trefoil Factor 2 Regulates Proliferation and Apoptosis of Pancreatic Cancer Cells and LPS-Induced Normal Pancreatic Duct Cells by β-Catenin Pathway. Cancer management and research, 2020. 12: p. 10705–10713. [PubMed: 33149677]
23. Thiem S, et al. , Inducible gene modification in the gastric epithelium of Tff1-CreERT2, Tff2-rtTA, Tff3-luc mice. genesis, 2016. 54(12): p. 626–635. [PubMed: 27731922]
24. Belle NM, et al. , TFF3 interacts with LINGO2 to regulate EGFR activation for protection against colitis and gastrointestinal helminths. Nat Commun, 2019. 10(1): p. 4408. [PubMed: 31562318]
25. Hung LY, et al. , Trefoil Factor 2 Promotes Type 2 Immunity and Lung Repair through Intrinsic Roles in Hematopoietic and Nonhematopoietic Cells. Am J Pathol, 2018. 188(5): p. 1161–1170. [PubMed: 29458008]
26. Engevik KA, et al. , Trefoil factor 2 activation of CXCR4 requires calcium mobilization to drive epithelial repair in gastric organoids. J Physiol, 2019. 597(10): p. 2673–2690. [PubMed: 30912855]
27. Meyer zum Buschenfelde D, Tauber R, and Huber O, TFF3-peptide increases transepithelial resistance in epithelial cells by modulating claudin-1 and −2 expression. Peptides, 2006. 27(12): p. 3383–90. [PubMed: 17018241]
28. Antunes MB, et al. , Murine nasal septa for respiratory epithelial air-liquid interface cultures. Biotechniques, 2007. 43(2): p. 195–6, 198, 200 passim. [PubMed: 17824387]
29. Cooper HS, et al. , Clinicopathologic study of dextran sulfate sodium experimental murine colitis. Lab Invest, 1993. 69(2): p. 238–49. [PubMed: 8350599]
30. Klopfleisch R, Multiparametric and semiquantitative scoring systems for the evaluation of mouse model histopathology--a systematic review. BMC Vet Res, 2013. 9: p. 123. [PubMed: 23800279]
31. Kennedy RJ, et al. , Interleukin 10-deficient colitis: new similarities to human inflammatory bowel disease. Br J Surg, 2000. 87(10): p. 1346–51. [PubMed: 11044159]
32. Suzuki R, et al. , Strain differences in the susceptibility to azoxymethane and dextran sodium sulfate-induced colon carcinogenesis in mice. Carcinogenesis, 2006. 27(1): p. 162–9. [PubMed: 16081511]
33. Mahe MM, et al. , Establishment of Gastrointestinal Epithelial Organoids. Curr Protoc Mouse Biol, 2013. 3(4): p. 217–40. [PubMed: 25105065]
34. Haber AL, et al. , A single-cell survey of the small intestinal epithelium. Nature, 2017. 551(7680): p. 333–339. [PubMed: 29144463]
35. Hsu YC, Li L, and Fuchs E, Transit-amplifying cells orchestrate stem cell activity and tissue regeneration. Cell, 2014. 157(4): p. 935–49. [PubMed: 24813615]
36. Rangel-Huerta E and Maldonado E, Transit-Amplifying Cells in the Fast Lane from Stem Cells towards Differentiation. Stem Cells Int, 2017. 2017: p. 7602951. [PubMed: 28835754]
37. Kohanski MA, et al. , Solitary chemosensory cells are a primary epithelial source of IL-25 in patients with chronic rhinosinusitis with nasal polyps. J Allergy Clin Immunol, 2018. 142(2): p. 460–469 e7. [PubMed: 29778504]
38. Workman AD, Kohanski MA, and Cohen NA, Biomarkers in Chronic Rhinosinusitis with Nasal Polyps. Immunol Allergy Clin North Am, 2018. 38(4): p. 679–692. [PubMed: 30342588]
39. Cai Y, et al. , Trefoil factor family 2 expression inhibits gastric cancer cell growth and invasion in vitro via interactions with the transcription factor Sp3. Int J Mol Med, 2016. 38(5): p. 1474–1480. [PubMed: 27668303]
40. Hanisch C, et al. , Trefoil factor 3 mediates resistance to apoptosis in colon carcinoma cells by a regulatory RNA axis. Cell Death Dis, 2017. 8(3): p. e2660. [PubMed: 28277538]
41. Le J, et al. , ITF promotes migration of intestinal epithelial cells through crosstalk between the ERK and JAK/STAT3 pathways. Sci Rep, 2016. 6: p. 33014. [PubMed: 27616044]
42. Lee RJ, et al. , Mouse nasal epithelial innate immune responses to Pseudomonas aeruginosa quorum-sensing molecules require taste signaling components. Innate Immun, 2014. 20(6): p. 606–17. [PubMed: 24045336]
43. DePoortere D, Chen B, and Cohen NA, Polyhydrated ionogen with MgBr2 accelerates in vitro respiratory epithelial healing. Am J Rhinol Allergy, 2013. 27(4): p. 333–7. [PubMed: 23883817]

44. Rani R, et al. , TGF-beta limits IL-33 production and promotes the resolution of colitis through regulation of macrophage function. Eur J Immunol, 2011. 41(7): p. 2000–9. [PubMed: 21469118]
45. Dubeykovskaya Z, et al. , Secreted trefoil factor 2 activates the CXCR4 receptor in epithelial and lymphocytic cancer cell lines. J Biol Chem, 2009. 284(6): p. 3650–62. [PubMed: 19064997]
46. Wu CS, et al. , Aberrant JAK/STAT Signaling Suppresses TFF1 and TFF2 through Epigenetic Silencing of GATA6 in Gastric Cancer. Int J Mol Sci, 2016. 17(9).
47. Pickert G, et al. , STAT3 links IL-22 signaling in intestinal epithelial cells to mucosal wound healing. J Exp Med, 2009. 206(7): p. 1465–72. [PubMed: 19564350]
48. Lavery DL, et al. , The stem cell organisation, and the proliferative and gene expression profile of Barrett's epithelium, replicates pyloric-type gastric glands. Gut, 2014. 63(12): p. 1854–1863. [PubMed: 24550372]
49. Koo BK and Clevers H, Stem cells marked by the R-spondin receptor LGR5. Gastroenterology, 2014. 147(2): p. 289–302. [PubMed: 24859206]
50. Wang W, et al. , Heat shock transcription factor 2 inhibits intestinal epithelial cell apoptosis through the mitochondrial pathway in ulcerative colitis. Biochemical and Biophysical Research Communications, 2020. 527(1): p. 173–179. [PubMed: 32446363]
51. Aamann L, Vestergaard EM, and Grønbæk H, Trefoil factors in inflammatory bowel disease. World journal of gastroenterology, 2014. 20(12): p. 3223–3230. [PubMed: 24696606]
52. Loncar MB, et al. , Tumour necrosis factor alpha and nuclear factor kappaB inhibit transcription of human TFF3 encoding a gastrointestinal healing peptide. Gut, 2003. 52(9): p. 1297–303. [PubMed: 12912861]
53. McBerry C, et al. , Trefoil factor 2 negatively regulates type 1 immunity against Toxoplasma gondii. J Immunol, 2012. 189(6): p. 3078–84. [PubMed: 22896633]
54. Barrera GJ, Sanchez G, and Gonzalez JE, Trefoil factor 3 isolated from human breast milk downregulates cytokines (IL8 and IL6) and promotes human beta defensin (hBD2 and hBD4) expression in intestinal epithelial cells HT-29. Bosn J Basic Med Sci, 2012. 12(4): p. 256–64. [PubMed: 23198942]
55. Tran CP, et al. , Trefoil peptide TFF2 (spasmolytic polypeptide) potently accelerates healing and reduces inflammation in a rat model of colitis. Gut, 1999. 44(5): p. 636–42. [PubMed: 10205199]
56. Soriano-Izquierdo A, et al. , Trefoil peptide TFF2 treatment reduces VCAM-1 expression and leukocyte recruitment in experimental intestinal inflammation. J Leukoc Biol, 2004. 75(2): p. 214–23. [PubMed: 14597729]
57. Xu K, et al. , Crystal structures of Lgr4 and its complex with R-spondin1. Structure, 2013. 21(9): p. 1683–9. [PubMed: 23891289]
58. Liu S, et al. , Lgr4 gene deficiency increases susceptibility and severity of dextran sodium sulfate-induced inflammatory bowel disease in mice. J Biol Chem, 2013. 288(13): p. 8794–803; discussion 8804. [PubMed: 23393138]
59. Onozato D, et al. , Generation of Intestinal Organoids Suitable for Pharmacokinetic Studies from Human Induced Pluripotent Stem Cells. Drug Metab Dispos, 2018. 46(11): p. 1572–1580. [PubMed: 29615438]
60. Wendt MK, et al. , Down-regulation of epithelial cadherin is required to initiate metastatic outgrowth of breast cancer. Mol Biol Cell, 2011. 22(14): p. 2423–35. [PubMed: 21613543]
61. Hahn S, et al. , Organoid-based epithelial to mesenchymal transition (OEMT) model: from an intestinal fibrosis perspective. Sci Rep, 2017. 7(1): p. 2435. [PubMed: 28550311]
62. Bates RC and Mercurio AM, Tumor necrosis factor-alpha stimulates the epithelial-to-mesenchymal transition of human colonic organoids. Mol Biol Cell, 2003. 14(5): p. 1790–800. [PubMed: 12802055]
63. Mi S, et al. , LINGO-1 is a component of the Nogo-66 receptor/p75 signaling complex. Nat Neurosci, 2004. 7(3): p. 221–8. [PubMed: 14966521]
64. Pepinsky RB, et al. , Structure of the LINGO-1-anti-LINGO-1 Li81 antibody complex provides insights into the biology of LINGO-1 and the mechanism of action of the antibody therapy. J Pharmacol Exp Ther, 2014. 350(1): p. 110–23. [PubMed: 24756303]

65. Inoue H, et al. , Inhibition of the leucine-rich repeat protein LINGO-1 enhances survival, structure, and function of dopaminergic neurons in Parkinson’s disease models. Proc Natl Acad Sci U S A, 2007. 104(36): p. 14430–5. [PubMed: 17726113]

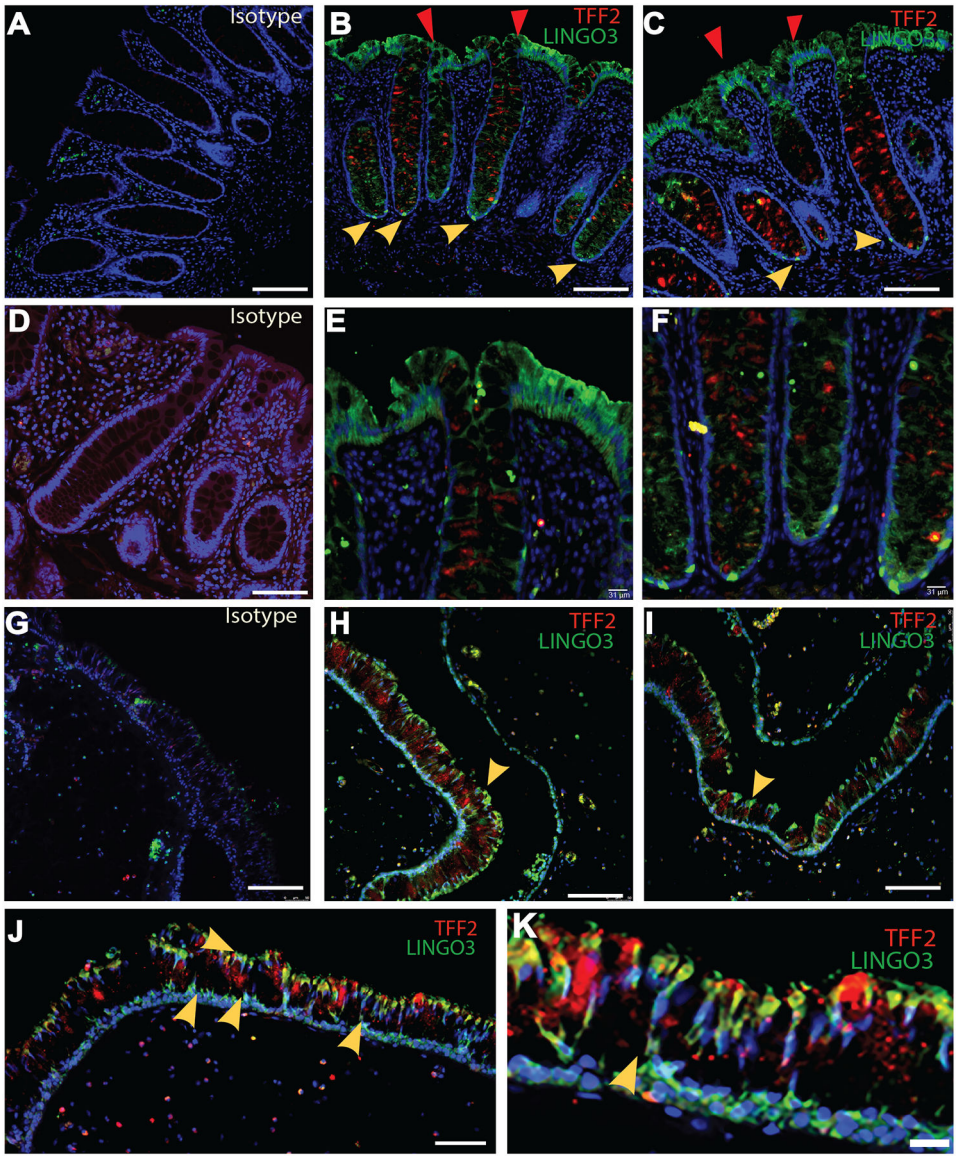

Figure 1.

LINGO3 is expressed on mucosal epithelia of human tissues. (A-F) Double immunofluorescence staining using anti-TFF2Ab (red) and anti-LINGO3 Ab (green) vs. (A, D) isotype matched Ab on human rectum (A-C: Magnification at 32x, D-F: 32x with digital zoom, respectively). Red arrows depict LINGO3 expression on apical side of the tissue while yellow depict LINGO3 expression at the base of intestinal crypts. (G-K) Staining (H-K) or Isotype negative control (G) on human nasal polyps (G-J: Magnification 20x, K: 20x with digital zoom, respectively). Yellow arrows depict LINGO3 expression at the base of the nasal polyps. Mean ± SEM from n=2–6 samples shown. 2–3 independent experiments performed.

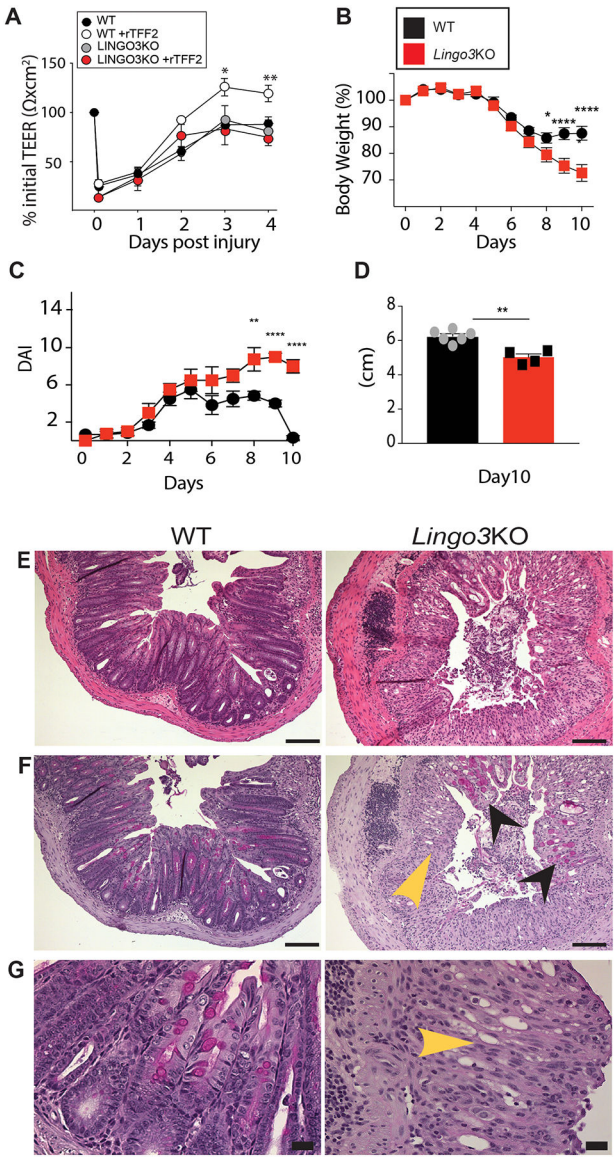

Figure 2.

LINGO3 deficiency results in poor recovery from mucosal epithelial injury. (A) Transepithelial resistance (TEER) of primary WT and LINGO3 KO nasal epithelial cells following rTFF2 (10μg/mL) or 1x PBS treatment. Following treatment of 2.5% DSS in drinking water (0–5days) and withdrawal (6–10 days), (B) Percent change in body weight (C) disease activity score (DAI) and (D) Colon lengths (cm) on day 10 of WT and LINGO3 KO mice. (E) H&E- and (F,G) PAS-stained colon sections at 10 days, 5 days following cessation of DSS (E, F: 10x, G: 40x magnification). Black arrowheads label remaining goblet cells within damaged LINGO3 LO intestinal tissue. Yellow arrowheads indicate loss of goblet cells and normal tissue architecture in KO samples. Mean ± SEM from n=4–6 samples (A) or mice/genotype (B-G). 2–3 independent experiments. *p ≤ 0.05, ** p ≤0.005, **** p ≤ 0.0001

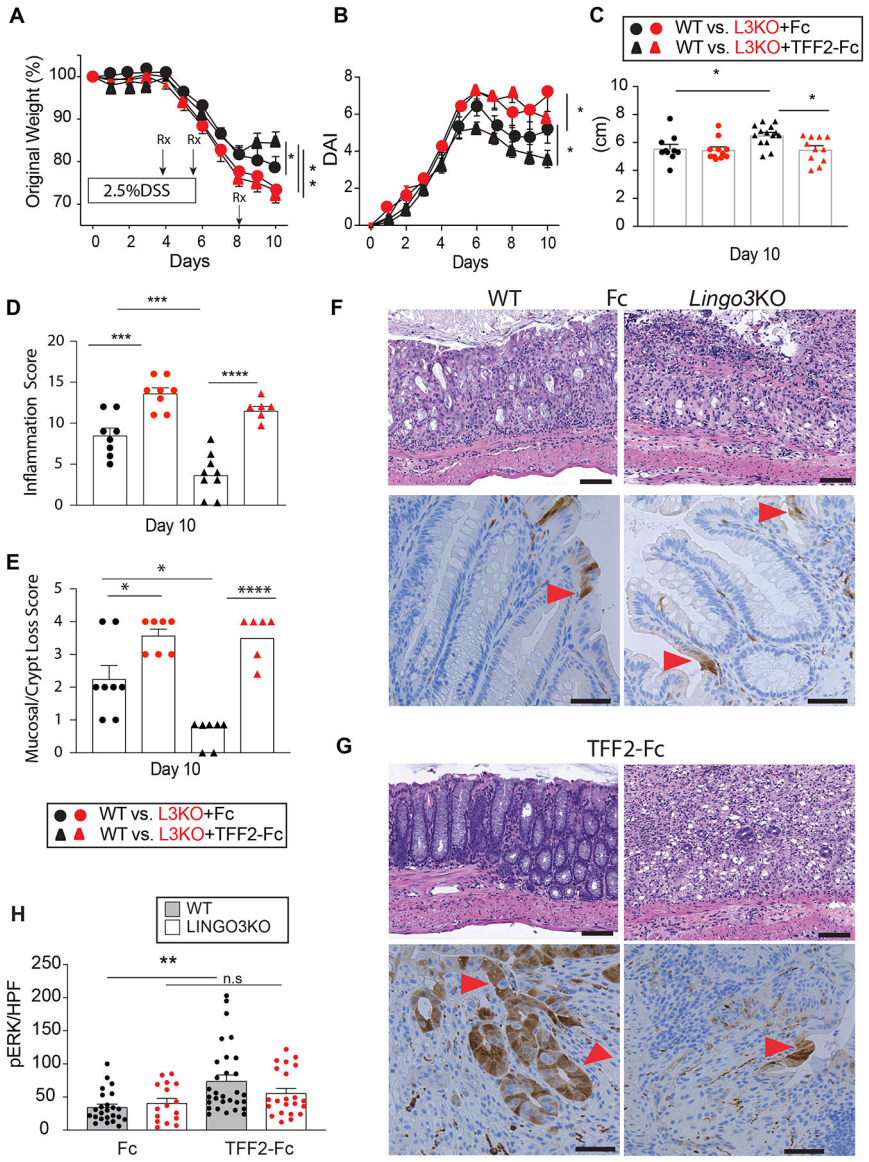

Figure 3.

TFF2-Fc treatment requires LINGO3 KO to accelerate healing post DSS-colitis. (A) Change in body weight and (B) disease activity score (DAI) following therapeutic administration of Fc or TFF2-Fc at the timepoints indicated following oral administration of 2.5% DSS in LINGO3 KO and WT mice, as well as (C) Colon length (cm) (D) Inflammation score (E) Mucosal/crypt loss score in tissue collection on day 10. H&E (top) and pERK1/2 (bottom) stained images of colon following (F) control Fc or (G) TFF-Fc treatment 10 days post 2.5% DSS (Magnification 20x) and (H) quantification of $pERK^{+}$ cells per high powerfield (HPF) for those treatment groups. Red arrowheads indicate pERK1/2+ cells, brown. Mean ± SEM from n=4–6 mice/genotype. 3 independent experiments. * $p \leq 0.05$, ** $p \leq 0.005$, *** $p \leq 0.0005$, **** $p \leq 0.0001$

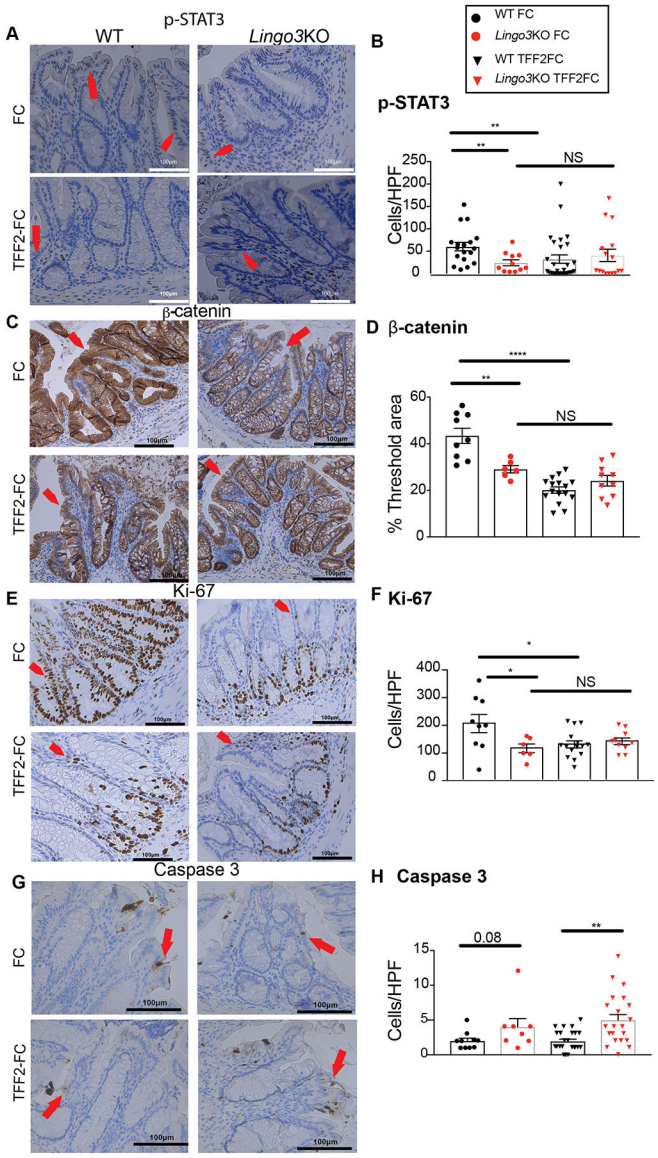

Figure 4.

TFF2-Fc mediated signaling cascades are only partially dependent upon LINGO3. Colon tissue from WT or LINGO3 KO mice was collected at 10 days post 2.5% DSS administration combined with TFF2-Fc or Fc treatment and immunostained for (A,B) phosphorylated (p)-STAT3, (C,D) β-catenin, (E,F) proliferative cell marker Ki-67, and (G,H) apoptotic cell marker cleaved caspase 3. (A,C,E,G) are respective representative images (Magnification 20x). (B,F,H) are quantification of + cells per high powerfield for the respective markers and (D) is percent of threshold area for β-catenin. Red arrowheads indicate positively stained cells or tissue regions, in brown. Mean ± SEM from n=4–6 mice/ genotype/ 4 images per mouse. 2–3 independent experiments. * $p \leq 0.05$, ** $p \leq 0.005$, *** $p \leq 0.0005$, **** $p \leq 0.0001$

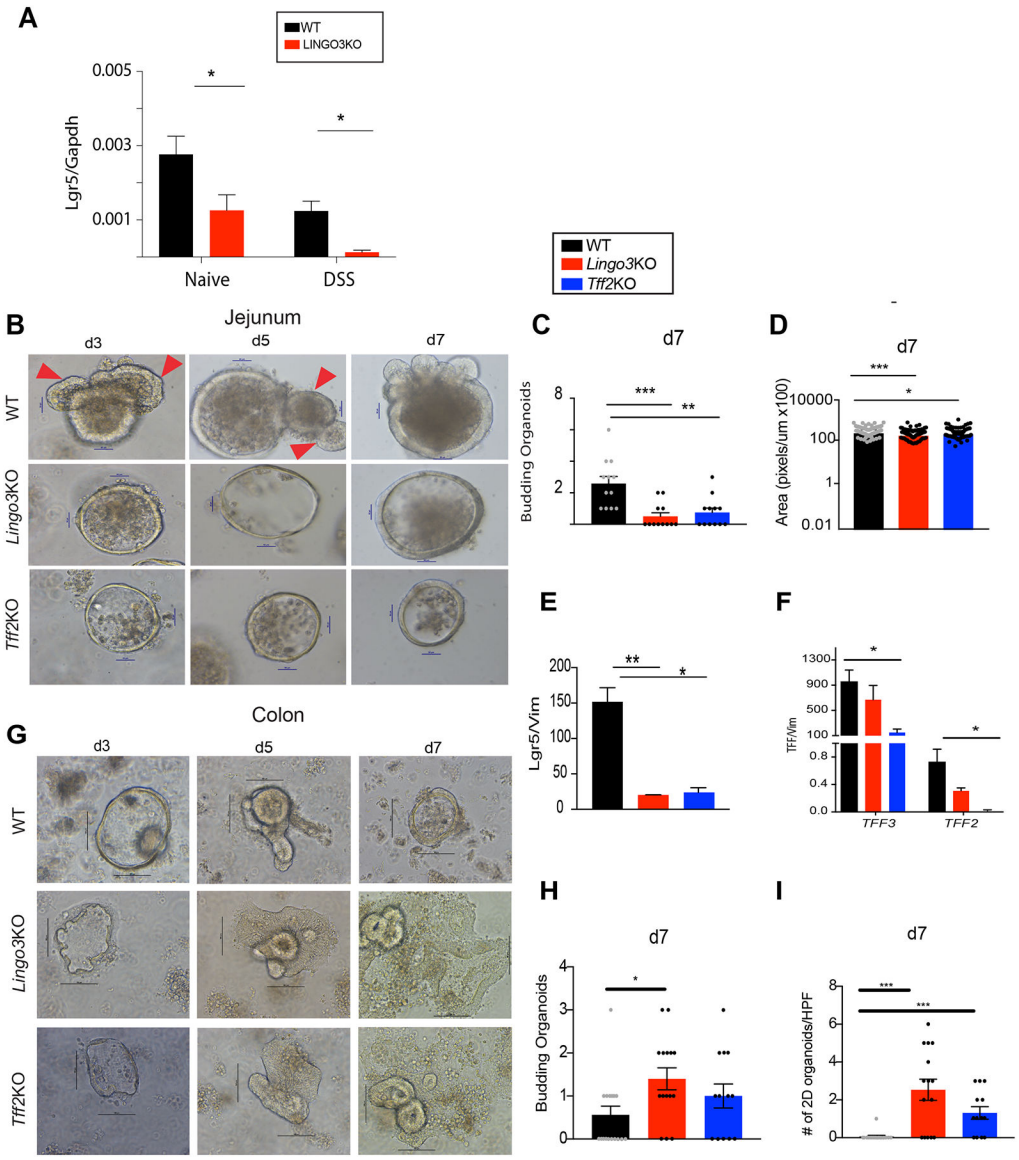

Figure 5.

LINGO3 deficiency causes perturbations in intestinal stem cell activity. (A) *Lgr5* mRNA expression in colons from naïve or day 10 post 2.5% DSS administration. (B) Intestinal organoid culture or (G) colonic organoid culture from WT LINGO3 KO, TFF2 KO mouse strains, brightfield images taken at days 3, 5, 7 (magnification 20x). Arrows point to buds. Number of budding organoids per genotype at day 7 of culture for (C) intestinal organoids and (H) colonic organoids. Intestinal organoid (D) Area (pixels/um) (E) *Lgr5*, (F) *Tff3* and *Tff2* mRNA at day 7 of culture. (I) Number of 2D colonic organoids for each genotype. (Mean ± SEM from n=4–6 mice/genotype. 2–3 independent experiments. * p ≤ 0.05, ** $p \leq$ 0.005, *** p ≤ 0.0005,

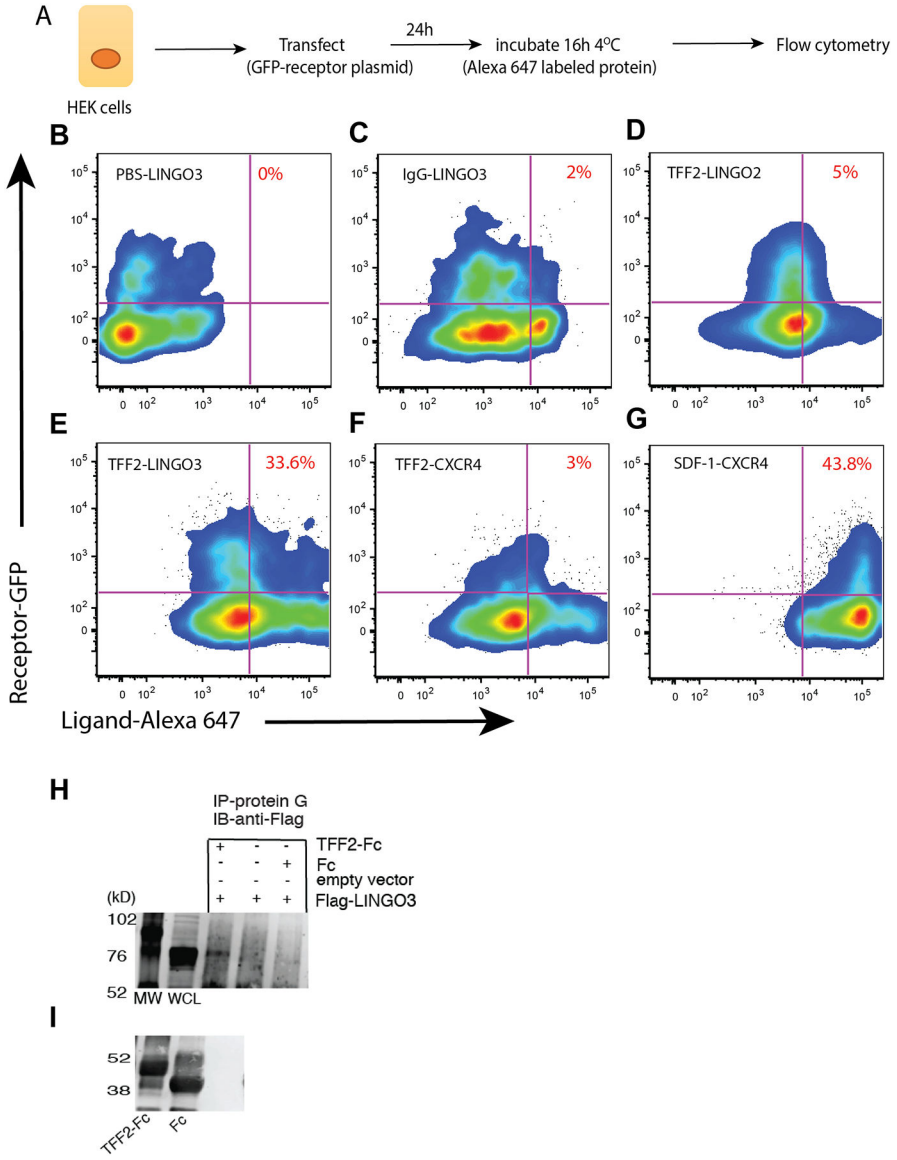

Figure 6.

TFF2 has weak affinity interactions with LINGO3. (A) Approach for incubation of soluble ligand with transfected HEK cells followed by flow cytometry to identify doubly fluorescent cells. Percent of doubly fluorescent cells identified in the upper right quadrant for LINGO3-GFP transfectants incubated with (B) PBS (C) IgG-Alexa Fluor 647 or (E) TFF2- Alexa Fluor 647. (D) LINGO2-GFP transfected HEK cells incubated with TFF2-Alexa Fluor 647. (F) CXCR4-GFP transfectants incubated with (F) TFF2-Alexa Fluor 647 or (G) SDF1-Alexa Fluor 647, a known high affinity binding partner. (H) Coimmunoprecipitation of Flag-LINGO3 and TFF2-Fc in transfected CHO cells. (I) Control TFF2-Fc and Fc without co-immunoprecipitation migrate at 50 kD and 40 kD.